

Effects of Surface Roughness
On an Airfoil
MCE 414 Laboratory Report V

Performed by:

Team 14: Aidan Votaw, Natalie Dmoch, Seth Mace, Donnie Blanpied,
Corey Murphy

December 12, 2018

Arun Shukla, Yi Zheng

Department of Mechanical, Industrial, and Systems Engineering
University of Rhode Island

Abstract

The purpose of this experiment was to observe and measure the effects on the dynamics of an airfoil by changing the surface roughness of the airfoil. This was done by 3D printing an airfoil using PLA and attaching varying grits of sandpaper to the airfoil. Tests were taken with grits of 60, 120, 180, and 320. For each grit, the following was done; a pitot-static tube was lowered in height increments of 0.2 inches while recording pressure at each position at speeds of 400, 600, 800 and 1,000 RPM. The coefficient of lift for 60, 120, 180 and 320 grit sandpaper for 400 RPM were found to be 0.00027, 0.0177, 0.0491 and 0.0601; the coefficient of drag was 0.027556, 0.022964, 0.032149 and 0.02526. For 600 RPM, the coefficient of lift was 0.01968, 0.017006, 0.051018 and 0.077742; the coefficient of drag was 0.016023, 0.01735, 0.029597 and 0.01837. For 800 RPM, the coefficient of lift was 0.028014, 0.030748, 0.060129 and 0.080627; the coefficient of drag was 0.020323, 0.016649, 0.02526 and 0.016074. Finally, for 1,000 RPM, the coefficient of lift was 0.036893, 0.041812, 0.072803 and 0.096415; the coefficient of drag was 0.024385, 0.018599, 0.023558 and 0.021078.

Contents

1	Introduction	1
2	Theory	1
3	Experimental Apparatus and Procedures	4
4	Presentation of Results	6
5	Discussion of Results	9
6	Conclusions and Recommendations	10
7	Acknowledgements	10
8	Appendices	13

List of Figures

1	Surface roughness analyzer.	1
2	Aerodynamic Diagram of an airfoil, from the lab handout [2].	2
3	Solidworks render of airfoil.	4
4	Airfoil in wind tunnel.	4
5	Wind tunnel speed controller.	5
6	Device used to record pressure of air.	6
7	Coefficient of Lift	7
8	Coefficient of Drag	8
9	Coefficient of Skin Friction	8

List of Tables

1	Data at 400 RPM	6
2	Data at 600 RPM	6
3	Data at 800 RPM	7
4	Data at 1000 RPM	7
5	Surface Roughness of Sandpaper	9
6	Surface Roughness of Airfoil	9

Nomenclature

μ . .	Dynamic viscosity	Pa · s
ρ . .	Fluid density	$\frac{kg}{m^3}$
τ_{wall}	Shear stress at the airfoil	Pa
A . .	Cross-sectional area of the wind-tunnel	m^2
A . .	Wing platform / Surface area of the wing	m^2
$C_{D,L}$	Characteristic coefficient of lift and drag	—
C_F .	Coefficient of skin friction	—
D_H .	Hydraulic diameter	m
$F_{D,L}$	Lift and drag force	N
p_{stat}	Static Pressure	Pa
p_{tot} .	Total Pressure	Pa
P_{wet}	Wet-perimeter of the wind-tunnel	m
R_a .	Average surface roughness	—
R_t .	Distance from the absolute highest point to the absolute lowest point	—
Re .	Reynolds number for flow in a pipe	—
V . .	Fluid velocity	$\frac{m}{s}$
V_{FS} .	Free stream velocity	$\frac{m}{s}$

1 Introduction

An Airfoil is defined as a cross sectional shape of a wing designed to go through a fluid in order to produce aerodynamic force. This force has two components, lift and drag. Lift is a force that acts in a perpendicular direction to the body, with respect to the fluid velocity. Drag is the force that acts in a parallel direction with respect to fluid velocity. In the example of a airplane wing, the lift would be the force acting to raise the plane off the ground. The drag would be the force opposing the engines of the plane, and opposing the movement of the plane in a forward direction. These two forces are produced because of pressure differences above and below an object, in the case of this lab, an airfoil. The fluid that passes over the airfoil in this lab will be room temperature air. The air will be driven by a wind tunnel. This lab focuses on the relationship between pressure observed above and below an airfoil as a function of air velocity, surface roughness.

Surface roughness can be thought of deviation from a perfectly flat surface. These deviations, seen as peaks and valleys, are often called asperities. The roughness is measured in a few ways. First is the average roughness or, R_a . This is an average value found over a sample size of material. Another is the total range R_f . This value is seen as a total difference of the highest point to the lowest point in a sample size. In this lab, the surface roughness values are found experimentally using a Mahr-Federal Surfanalyser, seen in Figure . Surface roughness has a direct impact on friction, Therefore would effect the dynamics of airflow around the airfoil. This lab will investigate this effect.



Figure 1: Surface roughness analyzer.

2 Theory

An airfoil immersed within a flowing stream of fluid is subjected to aerodynamic forces resulting from the pressure acting on the airfoil surface and interactions from viscosity. These aerodynamic forces can be resolved into two components: lift and drag. Lift acts on the airfoil perpendicular to the relative velocity of the fluid while drag acts on the airfoil parallel to the relative velocity of the fluid. The main purpose of an airfoil is to create substantially more lift than drag. To do this, the airfoil is designed in such a way that the incoming fluid is

diverted across a longer path on the top side than the fluid on the bottom side. This causes the fluid on the top to move at a higher velocity than the fluid on the bottom. A simplified free body diagram of these forces acting on an airfoil, or wing can be seen in Figure 1.

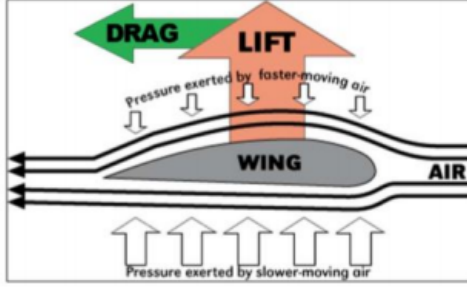


Figure 2: Aerodynamic Diagram of an airfoil, from the lab handout [2].

Referencing Bernoulli's Principle which states that an increase in the speed of a fluid occurs simultaneously with a decrease pressure, the top of the airfoil would have a lower fluid pressure than the bottom. The higher pressure on the bottom creates the lift force component, lifting the airfoil upwards. These lift and drag components produced by an airfoil are most affected by the airfoils geometry, the angle relative to the fluid flow (angle of attack) and the velocity relative to the fluid flow. As the angle of attack increases, the lift produced by the airfoil tends to increase with it until a certain point known as the critical angle of attack. At the critical angle of attack, the airfoil begins to produce much more drag and much less lift, reversing the previous trend. The reversal at this point is called turbulence, which can cause violent movement of the airfoil.

This experiment focuses on the dynamics of an airfoil due to changes in thrust and angle of attack. In order to measure the dynamic pressure or difference between the total pressure and static pressure, a pitot-static tube must be used to measure pressures at various heights relative to the airfoil. The total pressure is calculated using the equation:

$$p_{tot} = p_{stat} + \frac{\rho V^2}{2} \quad (1)$$

where p_{tot} is the total pressure, p_{stat} is the static pressure, ρ is the density of the fluid, and V is the velocity relative to the fluid. This pressure differential between the top and bottom faces of the airfoil cause a "lifting" force to act along the side of higher pressure.

As seen in Eq. 1, the pressure differential is dependent on the fluid velocity. Additionally in relation to the velocity, the Reynold's number Re is also an important quantity to be considered for an airfoil, as it defines whether the flow of a fluid is laminar or turbulent. As seen in the equation below,

$$Re = \frac{\rho V_{FS} D_H}{\mu} \quad (2)$$

Where the hydraulic diameter, D_H is defined as:

$$D_H = \frac{4A}{P_{wet}} \quad (3)$$

where ρ is the density of the fluid, V_{FS} is the free stream velocity and μ is the dynamic viscosity of the fluid.

Determining if the fluid flow is turbulent or not is an important factor when dealing with an airfoil. A turbulent flow, corresponding to a higher Reynold's number, may result in a significant decrease in lift and consequently an increase in drag. The coefficient of drag and lift $C_{D,L}$ is a dimensionless quantity for lift and drag forces acting on an airfoil. This is defined in the equation below:

$$C_{D,L} = \frac{2F_{D,L}}{\rho V_{FS}^2 A} \quad (4)$$

where $F_{D,L}$ is the force of lift or drag, ρ is the density of the fluid and V_{FS} is the free stream velocity. It is important to note that these coefficients are two separate quantities and thus do not share the same value. The drag force F_D is a parallel generated force in the direction of the relative velocity of the fluid.

As stated previously, a higher Reynolds number corresponds to higher drag values. This is due to shear stress acting on the surface of the airfoil from the friction of the fluid, known as skin friction. The skin friction generated along the surface of an airfoil C_f , can be defined as,

$$C_f = \frac{2\tau_{wall}}{\rho V_{FS}^2} \quad (5)$$

where τ_{wall} is the shear stress at the airfoil, ρ is the density of the fluid and V_{FS} is the free stream velocity.

The dynamic pressure data collected from the pitot-static tube will be used to analyze the effect of different surface roughness values of the airfoil on the coefficient of drag. To create varying surface roughness values, different grits of sandpaper will be fit and adhered to the airfoil. Surface roughness can be thought of as a derivation of a perfectly flat surface. These derivations are the peaks and valleys that are seen on the surface profile, called asperities. Surface roughness can be represented using two different calculations. For the purpose of this lab, a surface roughness measurement machine will be used, however it is still important to understand the concepts of surface roughness. The first measurement is called the center line average or average surface roughness, R_a , which is represented in the equation below:

$$R_a = \frac{1}{L} \int_{x=0}^{x=L} |z| dx \quad (6)$$

The variable L is the total length of the sample's surface and z is the distance from the center line to the asperity peak or valley. The second measurement is the calculated total

difference of the highest asperity point to the lowest asperity point in a surface sample, R_f . Both of these values are collected from the Mahr-Federal Surfanalyser for the airfoil itself and the four grits of sandpaper. These values can be analyzed against the corresponding pressure data and calculated coefficients of drag and lift to see the effect of surface roughness.

3 Experimental Apparatus and Procedures

In this experiment, the pressures around an airfoil were measured and observed as a function of surface roughness. The airfoil, as seen in Figures 2 and 3, was created using additive manufacturing. The Raise N-2 3D printer was used with standard PLA filament to print the foil design. Initially the foil was printed vertically, however it was found after multiple failed attempts that a horizontal orientation was the most successful.

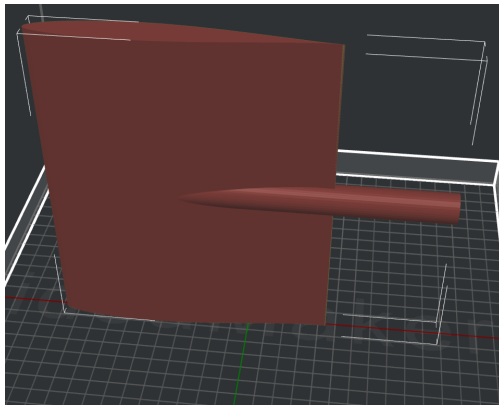


Figure 3: Solidworks render of airfoil.



Figure 4: Airfoil in wind tunnel.

The varying surface roughness was accomplished by adhering sandpaper with a range of

grits. These grits were 60, 120, 180, and 320. To find the surface roughness R_a and R_f values the Mahr-Federal Surfanalyser was used. To operate this machine, the sample is secured under the sensor probe. The probe is then lowered onto the sample and a surface profile is taken. The machine then calculates the R_a and R_f values. The surface profiles of the airfoil and the sandpaper was evaluated to find the average roughness, and the total range of asperities.

Each of the sandpaper grits, as well as the airfoil without sandpaper, were subjected to four different speeds in the wind tunnel; 400, 600, 800, and 1000 RPM. Speed of the wind tunnel was controlled via the controller as seen in Figure 5. The air pressure was then measured using the pitot-static tube and read on the device seen in Figure 6. The pitot-static tube started at a height 2 inches above the airfoil then, was lowered in increments of 0.2 inches until it was set at 2 inches below the trailing edge of the airfoil. The data collection was done via DAQ from a force-balance device and a pitot-static tube. The pitot tube measured pressure downstream of the airfoil. It is important to note that the airfoil was continually watched for any signs of it coming loose.



Figure 5: Wind tunnel speed controller.



Figure 6: Device used to record pressure of air.

4 Presentation of Results

Tables 1, 2, 3 and 4 show the data that was obtained for all sandpaper grits at 400, 600, 800 and 1000 RPM.

Table 1: Data at 400 RPM

Grit of Sandpaper	Drag Force	Lift Force	Coefficient of Lift C_L	Coefficient of Drag C_D	Coefficient of Skin Friction C_F
60	0.0749	0.00074	0.00027	0.027556	0.047239
120	0.0624	0.0483	0.0177	0.022964	0.039366
180	0.0874	0.1338	0.0491	0.032149	0.055112
320	0.0687	0.1635	0.0601	0.02526	0.043303

Table 2: Data at 600 RPM

Grit of Sandpaper	Drag Force	Lift Force	Coefficient of Lift C_L	Coefficient of Drag C_D	Coefficient of Skin Friction C_F
60	0.0980622	0.1204308	0.019678	0.016023	0.027469
120	0.106182	0.104076	0.017006	0.01735	0.029743
180	0.181134	0.312228	0.051018	0.029597	0.050738
320	0.112428	0.475776	0.077742	0.01837	0.031493

Table 3: Data at 800 RPM

Grit of Sandpaper	Drag Force	Lift Force	Coefficient of Lift C_L	Coefficient of Drag C_D	Coefficient of Skin Friction C_F
60	0.2211084	0.304794	0.028014	0.020323	0.034839
120	0.181134	0.33453	0.030748	0.016649	0.02854
180	0.274824	0.654192	0.060129	0.02526	0.043303
320	0.174888	0.877212	0.080627	0.016074	0.027556

Table 4: Data at 1000 RPM

Grit of Sandpaper	Drag Force	Lift Force	Coefficient of Lift C_L	Coefficient of Drag C_D	Coefficient of Skin Friction C_F
60	0.368514	0.55755	0.036893	0.024385	0.041802
120	0.28107	0.63189	0.041812	0.018599	0.031883
180	0.356022	1.100232	0.072803	0.023558	0.04038
320	0.318546	1.457064	0.096415	0.021078	0.036134

Figure 7 shows the coefficient of lift plotted for varying turbine speeds and sandpaper grits.

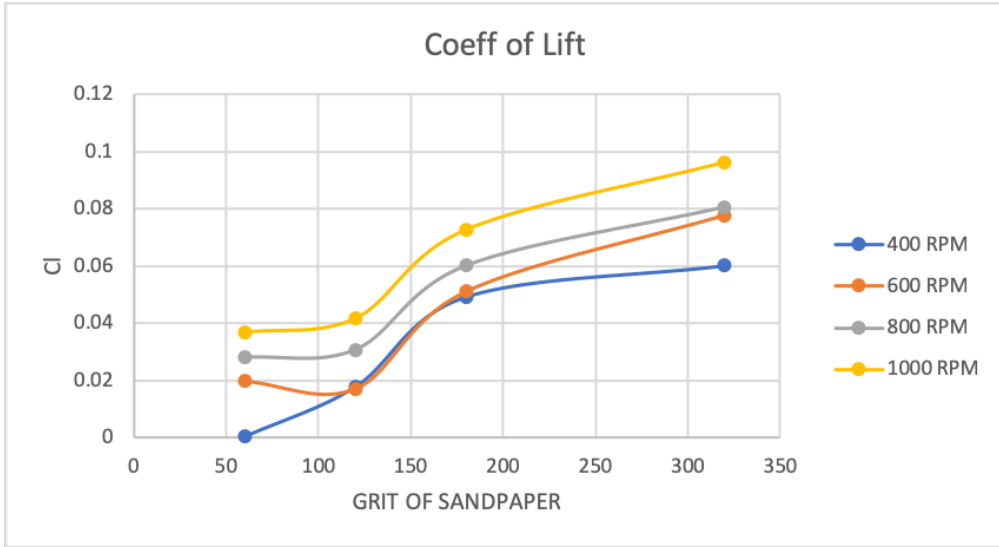


Figure 7: Coefficient of Lift

Figure 8 shows the coefficient of drag plotted for varying turbine speeds and sandpaper grits.

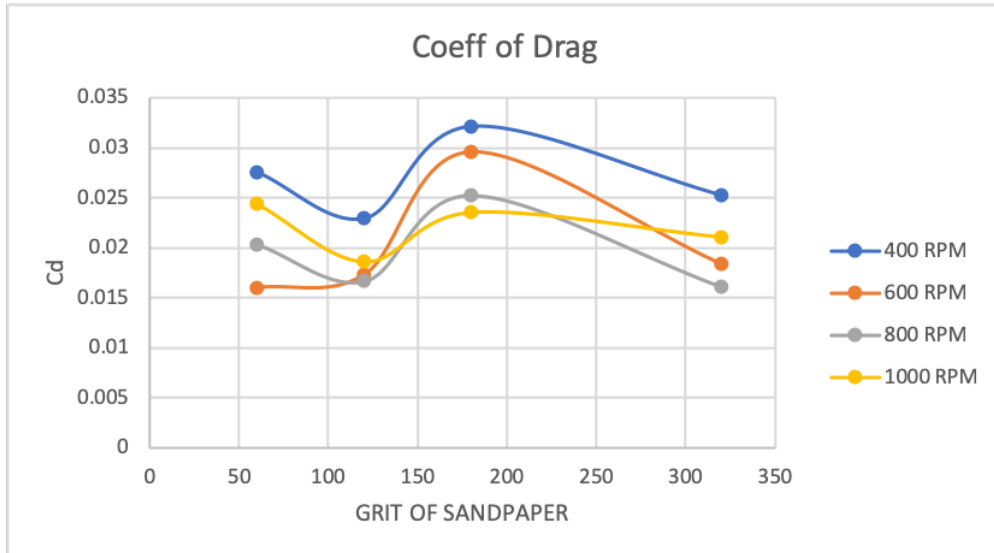


Figure 8: Coefficient of Drag

Figure 9 shows the coefficient of skin friction plotted for varying turbine speeds and sandpaper grits.

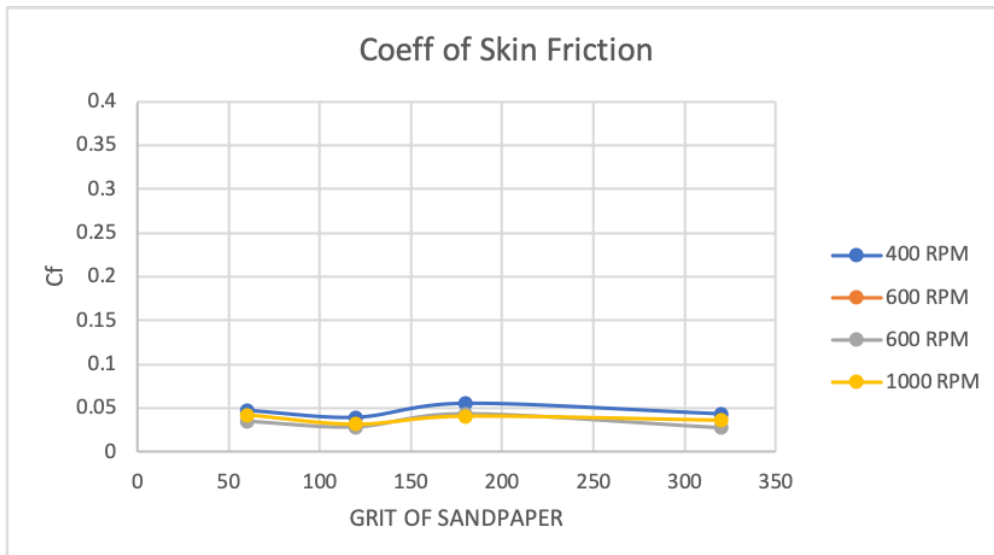


Figure 9: Coefficient of Skin Friction

Table 5 shows the tested surface roughness of each grit of sandpaper using tools provided by Meredith Westner.

Table 5: Surface Roughness of Sandpaper

Grit of Sandpaper	R_a μm	R_t μm
60	24.29	144.62
120	20.88	138.45
180	11.16	72.41
320	7.33	64.07

Table 6 shows the measured surface roughness of the 3D printed airfoil.

Table 6: Surface Roughness of Airfoil

	R_a μm	R_t μm
Underside Bottom Surface	36.92	207.74
Underside Top Surface	16.73	139.29
Top Side Smooth Surface	13.17	92.27

5 Discussion of Results

Before this experiment, it was hypothesized that the coefficient of lift and drag would increase as the surface roughness of the airfoil increased. After conducting this experiment, the data that was obtained seemed to go against the hypothesis. It would be expected that the 60 grit sandpaper due to the fact that it was the roughest sandpaper that was tested, would have the largest values of lift and drag coefficients, however, the 180 and 320 grit sandpapers consistently showed higher values over the 60 grit sandpaper.

When examining the coefficient of lift and drag for 400-1,000 RPM between 60-320 grit of sandpaper, there are inconsistencies between theory and obtained values. With increasing roughness of an airfoil, the coefficient of drag should be higher, however, this does not seem to be the case. In table 1, the coefficient of drag for 180 grit sandpaper is 0.032149 which is higher than the coefficient of drag for 60 and 120 grit paper. In table 2, the coefficient of drag, again, for 180 grit sandpaper came out to 0.029597 which is also higher than 60 and 120 grit sandpaper. This trend continues as seen in table 3 and in table 4.

Using the Mahr-Federal Surfalyzer, the surface roughnesses of the 60-320 grit sandpaper were determined as well as the surface roughness of the airfoil on both the top and bottom surface. It was necessary to calculate the surface roughness of the bottom because the airfoil was 3D printed horizontally with a raft that had to be sanded down, producing a coarser surface. Table 5 represents the calculation of surface roughness of 60-320 grit sandpaper. The team hypothesized that the lower the grit of sandpaper, the higher the R_a and R_t values. This is seen by comparing 60 grit sandpaper, which has an R_a value of 24.29 micrometers and an R_t of 144.62 micrometers, and 320 grit sandpaper which has an R_a value of 7.33 micrometers and an R_t of 64.07 micrometers. As stated, the 60 grit sandpaper had much greater surface roughness over that of the other sandpapers, and the roughness decreased as the grit of sandpaper increased, which was to be expected. With these results,

it was expected that the coefficient of drag forces would be proportional, meaning that the highest forces would be seen with the 60 grit sandpaper. As stated previously, this was not the case. The airfoil was wrapped in the sandpaper and the sandpaper was adhered to the airfoil by using duct-tape. This was not a perfect adhesion and at times, the sandpaper started to not adhere completely to the airfoil. This would have impacted the results, since it changed the dimensions of the airfoil, which is a possible form of error that could be the reason for the variance.

6 Conclusions and Recommendations

The purpose of this experiment is to better understand the effects of surface roughness on flow over airfoils. First, an airfoil was 3D printed using PLA. In order to measure the effects of an airfoil with varying surface roughness, 60, 80, 120 and 320 grit sandpaper was wrapped around the exterior of the airfoil. Each set of sandpaper on the airfoil was placed in the wind tunnel with speeds of 400, 600, 800 and 1,000 RPM. Air pressure for each sandpaper and speed was documented for data analysis. The data for grit per wind tunnel speed is seen in Figures 7, 8 and 9. This data represents corresponding drag and lift forces as well as coefficient of lift, drag and skin friction.

An additional measurement taken that contributed to analysis was measuring the roughness of each piece of sandpaper using the Mahr-Federal Surfalyzer. Due to the fact that the airfoil has a curved shape, the team measured the top of both the smooth (top surface) and coarse (bottom surface) above the curve as well as the bottom of both surfaces below the curve to account for overall roughness. These values are depicted in tabular form in Table 6. The roughness calculated by the Surfalyzer between the top and bottom surfaces shows a high variation between the R_a and R_t values. This is due to the fact that the airfoil was printed horizontally on a raft, so the raft had to be sanded down which cause a much coarser surface.

When running this experiment, challenges were faced. The first challenge faced was 3D printing the airfoil. Initially, the airfoil was printed vertically several times but stopped halfway. The airfoil was then printed horizontally with a raft on the bottom to support the design. When the horizontal airfoil finished printing, the raft had to be removed which created a different surface roughness on the bottom compared to the smoother finish on the top. For the calculations of the airfoil wrapped in sandpaper in the wind tunnel, data-wise, it would be more beneficial to use a wider selection of sandpaper as well as obtain calculations for the angle of attack in order to obtain more data for analysis and further determine inconsistencies and corresponding aerodynamic effects.

7 Acknowledgements

The authors of this report would like to thank the Mechanical Engineering and Industrial Systems Department at the University of Rhode Island for providing the funds, resources

and functional equipment for this experiment. They would also like to thank the teaching assistants present during the labs for providing assistance when needed during an experiment.

Bibliography

- [1] White, Frank M. *Heat and Mass Transfer*. Addison-Wesley, 1994. Print.
- [2] Zheng, Yi, Dr. "Aerodynamic Forces: Dynamics of an Airfoil, MCE 414 Lab 3." *MCE 414 Experimentation Resources*. Sakai URI, 16. October 2018. Web.

8 Appendices

All work was stated in this report.